Polarization Characteristics of Single-Mode Fiber Couplers

CHIN-LIN CHEN AND WILLIAM K. BURNS, MEMBER, IEEE

Abstract—The polarization characteristics of fiber couplers made of birefringent single-mode fibers are studied. The effect of anisotropic interfiber coupling, fiber birefringence, angular misalignment of fibers, and twisting on the coupler characteristics are identified. The polarization characteristics of the couplers are compared with that of isolated uncoupled fibers of the same birefringence and length. The equivalent lumped element representations for three classes of fiber couplers are also presented.

I. Introduction

SINCE low-loss single-mode optical fibers have become available in long lengths, many communication links and sensor systems have been developed to take advantage of the properties offered by these fibers. Obviously, means must be found to monitor the optical beams guided by the fibers, to divide a beam into two or more paths, or to combine two or more beams into one. An optical directional coupler is a basic structure for achieving these objectives. Methods of etching and twisting [1]-[5], fusing [6], [7], or polishing [8], [9] have been reported to construct couplers from existing single-mode fibers. Couplers can also be formed by drawing preforms with a twin core [10], [11]. These couplers have been used in many fiber optic systems. For many applications, optical interferometric systems, for example, the polarization characteristics of the coupler are a crucial factor affecting the stability and sensitivity of the system. In this work, the polarization characteristics of single-mode fiber couplers will be studied.

For an ideal stress-free untwisted fiber with a perfectly circular core and cladding and a rotationally symmetric index profile, the LP_{01} mode is the lowest order mode in the weakly guiding approximation. The transverse electric field of the LP_{01} mode is linearly polarized along a direction and is independent of the azimuthal variable ψ, and the longitudinal electric field has $\sin\psi$ or $\cos\psi$ type variation [12]. For the ideal fibers under consideration, any two orthogonal directions may be chosen as the reference directions, and an LP_{01} mode with an arbitrary state of polarization (SOP) may be considered as the superposition of LP_{01} modes polarized along two reference directions. In reality, the core of a fiber is only nominally circular and can be subject to internal stress which results in induced birefringence [13], [14]. Thus, conceptionally, we may envision a fiber as having an elliptical core or an elliptical refractive index profile. It is natural to choose the directions of the major and minor axes of the ellipse as the reference directions. Except for polarization maintaining fibers, the major and minor axes differ only slightly, of the order of a few percent, so that the description in terms of LP_{01} modes remains a valid approximation. Now the LP_{01} mode polarized along the major axis propagates with a velocity slightly different from that polarized along the minor axis. Therefore, real single-mode fibers are double-moded with two nondegenerate LP_{01} modes. Let $\beta \pm \frac{1}{2}\Delta\beta$ be the propagation constants of the LP_{01} modes polarized along the major and minor axes, respectively. In the absence of any external perturbation, the evolution of the SOP in the fiber is a result of the interference of these two eigenmodes. It is customary to introduce the birefringent beat length $L_{BB} = 2\pi/\Delta\beta$ to characterize the birefringence of the fiber. If the fiber is additionally subjected to stress from bends or twists, additional birefringence is induced. These additional birefringences would cause coupling between the fiber eigenmodes just described, and thus affect the evolution of the SOP. The change of fiber birefringence due to bending and twisting has been studied by Ulrich *et al.* [15], [16], [18], and by Smith [17]. In summary then, the evolution of the SOP in a twisted and/or bent and birefringent single-mode fiber depends on $\Delta\beta$ and the rate of twisting and/or degree of bending of the fiber [19]-[22]. For single-mode fiber couplers, an additional factor is involved due to coupling between the fibers. In the next section, a coupled mode equation, containing these and other coupler parameters, is established to describe the evolution of the SOP. To facilitate general understanding and to illustrate the roles played by various parameters, three idealized classes of couplers with increasing complexity are studied in Sections III-V before the general case is considered. Instead of examining all possible variations of the output SOP as a function of the input SOP, we find it useful to use Jones' matrices to describe the relations between input and output SOP [23], [24]. From the Jones matrix, an equivalent lumped element representation (ELER) may be found for each path between input and output ports. All elements of these ELER's are identified and presented in Sections III-V.

For three idealized classes of couplers the Jones matrices are particularly simple and can be represented by products of unitary matrices and a constant representing power transfer. This implies that each path can be modeled by a rotator, a retarder, and an isotropic absorber [24]. We show that, in these idealized cases, the evolution of the SOP in the coupler is controlled primarily by the birefringence of the fiber and that the impact of interfiber coupling on the SOP is relatively small or

Manuscript received March 30, 1982; revised May 26, 1982.

C.-L. Chen is with the Catholic University of America, Washington, DC 20017 and the Naval Research Laboratory, Washington, DC 20375, on leave from the School of Electrical Engineering, Purdue University, West Lafayette, IN 47907.

W. K. Burns is with the Naval Research Laboratory, Washington, DC 20375.

zero. In the real couplers, then, our results imply that the impact of the interfiber coupling on the SOP is second order compared to the impact of the intrinsic fiber birefringence and the birefringences induced in the fibers in the process of fabricating the coupler.

II. Coupled-Mode Equations

We begin by considering a single twisted birefringent fiber. The axial direction of the fiber is chosen as the z-axis. Fig. 1(a) depicts the cross section of the fiber at z. An elliptical core is drawn to represent a birefringent fiber with either an elliptical core or an elliptical refractive index profile. For convenience, the directions along the major and minor axes are also used as the local coordinate system (u, v). Since the fiber may be twisted, the angle Φ between u-axis and a laboratory or stationary x-axis can be a function of z, i.e., $\Phi = \Phi(z)$. If the fiber is not twisted, the field in the fiber is the superposition of two orthogonal modes propagating with propagation constants $\beta \pm \frac{1}{2}\Delta\beta$

$$\boldsymbol{E}(r, \psi, z) = \hat{u}E_u(z) f_u(r, \psi) + \hat{v}E_v(z) f_v(r, \psi) \tag{1}$$

where $E_u(z)$ and $E_v(z)$ vary like $\exp(-j(\beta \pm \frac{1}{2}\Delta\beta) z)$ with constant amplitude, and $f_u(r, \psi)$ and $f_v(r, \psi)$ describe the distribution of the fields of LP_{01} modes polarized in u and v directions, respectively. For the nominally circular fibers discussed in this work, f_u and f_v are independent of ψ and $f_u \simeq f_v$. We will ignore these functions henceforth. If the fiber is twisted, (1) may be used to approximate the fields with the mode amplitudes $E_u(z)$ and $E_v(z)$ governed by a coupled-mode equation [22], [25]

$$\begin{bmatrix} E_u' \\ E_v' \end{bmatrix} = \begin{bmatrix} -j(\beta + \frac{1}{2}\Delta\beta) & \Phi' - K_p \\ -(\Phi' - K_p) & -j(\beta - \frac{1}{2}\Delta\beta) \end{bmatrix} \begin{bmatrix} E_u \\ E_v \end{bmatrix} \tag{2}$$

where a prime signifies differentiation with respect to z. Also included in (2) is the birefringence induced by twisting via the photoelastic effect of the fiber and it is represented by the term K_p [15]-[19]. The mode amplitudes E_u, E_v in the rotating coordinates are related to E_x, E_y in the stationary coordinates

$$\begin{bmatrix} E_x \\ E_y \end{bmatrix} = \begin{bmatrix} \cos\Phi & -\sin\Phi \\ \sin\Phi & \cos\Phi \end{bmatrix} \begin{bmatrix} E_u \\ E_v \end{bmatrix}. \tag{3}$$

The coupled-mode equation for E_x and E_y can be obtained by substituting (3) into (2)

$$\begin{bmatrix} E_x' \\ E_y' \end{bmatrix} = -j \begin{bmatrix} N_{xx} & N_{xy} \\ N_{yx} & N_{yy} \end{bmatrix} \begin{bmatrix} E_x \\ E_y \end{bmatrix} \tag{4}$$

where

$$N_{xx} = \beta + \tfrac{1}{2}\Delta\beta \cos 2\Phi \tag{5a}$$

$$N_{yy} = \beta - \tfrac{1}{2}\Delta\beta \cos 2\Phi \tag{5b}$$

$$N_{xy} = N_{yx}^* = \tfrac{1}{2}\Delta\beta \sin 2\Phi - jK_p. \tag{5c}$$

Equation (4) is exactly equivalent to the coupled-mode equation derived previously by Sakai and Kimura [20].

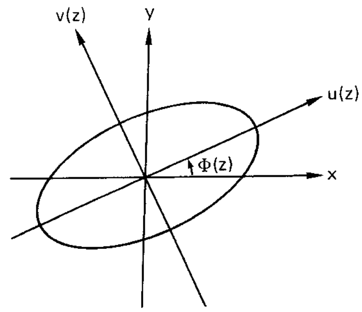

(a)

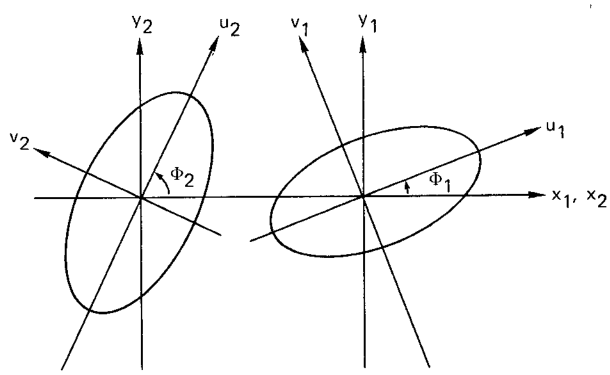

(b)

Fig. 1 (a) Cross section of a twisted birefringent fiber. (b) Cross section of a single-mode fiber coupler.

Now consider fiber couplers made of two nominally circular single-mode fibers [Fig. 1(b)]. A subscript 1 or 2 is added to the terms involved to identify the fiber involved. The coupled mode equation for the coupler can be obtained from (4) by adding terms representing the evanescent field coupling between fibers. Let K_x and K_y be the interfiber coupling constants pertaining to the interaction of E_{x1} with E_{x2}, and E_{y1} with E_{y2}, respectively [26]. Then, the coupled-mode equation for the couplers becomes

$$\begin{bmatrix} E_{x1}' \\ E_{y1}' \\ E_{x2}' \\ E_{y2}' \end{bmatrix} = -j \begin{bmatrix} N_{xx1} & N_{xy1} & K_x & 0 \\ N_{yx1} & N_{yy1} & 0 & K_y \\ K_x & 0 & N_{xx2} & N_{xy2} \\ 0 & K_y & N_{yx2} & N_{yy2} \end{bmatrix} \begin{bmatrix} E_{x1} \\ E_{y1} \\ E_{x2} \\ E_{y2} \end{bmatrix}. \tag{6}$$

If the spacing between fibers varies with z, so do K_x and K_y. In general, and even for couplers with uniform spacing, N_{xxi}, N_{yyi}, N_{yxi}, and N_{xyi} are z-dependent, except for couplers with nonbirefringent or untwisted fibers. Because of the presence of these z-dependent terms, it is difficult to treat (6) directly. However, it is convenient to transform (6) to the local (u, v) coordinate system by a simple substitution, which may be written as follows:

$$\tilde{E}_x = \tilde{T}(\Phi_1, \Phi_2)\tilde{E}_u \tag{7}$$

where

$$\tilde{E}_x = [E_{x1} \;\; E_{y1} \;\; E_{x2} \;\; E_{y2}]^t \tag{8a}$$

$$\tilde{E}_u = [E_{u1} \;\; E_{v1} \;\; E_{u2} \;\; E_{v2}]^t \tag{8b}$$

$$\tilde{T}(\Phi_1, \Phi_2) = \begin{bmatrix} \cos\Phi_1 & -\sin\Phi_1 & 0 & 0 \\ \sin\Phi_1 & \cos\Phi_1 & 0 & 0 \\ 0 & 0 & \cos\Phi_2 & -\sin\Phi_2 \\ 0 & 0 & \sin\Phi_2 & \cos\Phi_2 \end{bmatrix} \tag{9}$$

and the superscript t stands for the transpose of the matrix. Then (6) becomes

$$\tilde{E}_u' = -j[\tilde{B} + \tilde{C}]\,\tilde{E}_u \tag{10}$$

where

$$\tilde{B} = \begin{bmatrix} \beta_1 + \frac{1}{2}\Delta\beta_1 & j(\Phi_1' - K_{p1}) & K\cos(\Phi_1 - \Phi_2) & K\sin(\Phi_1 - \Phi_2) \\ -j(\Phi_1' - K_{p1}) & \beta_1 - \frac{1}{2}\Delta\beta_1 & -K\sin(\Phi_1 - \Phi_2) & K\cos(\Phi_1 - \Phi_2) \\ K\cos(\Phi_1 - \Phi_2) & -K\sin(\Phi_1 - \Phi_2) & \beta_2 + \frac{1}{2}\Delta\beta_2 & j(\Phi_2' - K_{p2}) \\ K\sin(\Phi_1 - \Phi_2) & K\cos(\Phi_1 - \Phi_2) & -j(\Phi_2' - K_{p2}) & \beta_2 - \frac{1}{2}\Delta\beta_2 \end{bmatrix} \tag{11}$$

$$\tilde{C} = \frac{\Delta K}{2}\begin{bmatrix} 0 & 0 & \cos(\Phi_1 + \Phi_2) & -\sin(\Phi_1 + \Phi_2) \\ 0 & 0 & -\sin(\Phi_1 + \Phi_2) & -\cos(\Phi_1 + \Phi_2) \\ \cos(\Phi_1 + \Phi_2) & -\sin(\Phi_1 + \Phi_2) & 0 & 0 \\ -\sin(\Phi_1 + \Phi_2) & -\cos(\Phi_1 + \Phi_2) & 0 & 0 \end{bmatrix} \tag{12}$$

and where $K = (K_x + K_y)/2$ and $\Delta K = K_x - K_y$. The coupler problem is solved by using (7) to transform the input $\tilde{E}_x(0)$ to $\tilde{E}_u(0)$, solving for $\tilde{E}_u(z)$ from (10) subject to the input condition $\tilde{E}_u(0)$, then finally transforming $\tilde{E}_u(z)$ to $\tilde{E}_x(z)$, which is the output of the coupler.

From (10), it is clear that for a given input SOP, the output SOP would depend on the birefringence $\Delta\beta_i$, twisting rate Φ_i' and K_{pi}, orientation Φ_i of the fibers, and the anisotropy of the interfiber coupling ΔK. The effects of these factors on the polarization characteristics of the fiber couplers will be considered in the following sections. Strictly speaking, $K_x \neq K_y$, as noted by Vanclooster and Phariseau [26]. For fibers commonly used in constructing couplers, $\Delta K \ll K$ [9]. Therefore, except in Section III, the terms associated with ΔK are ignored and (10) is greatly simplified.

If the fibers are highly birefringent, as represented by fibers with highly elliptical core or index profiles, for example, the field distribution $f_u(r, \psi)$ and $f_v(r, \psi)$ would be ψ-dependent. The interfiber coupling terms K_x and K_y in (6) would also be functions of Φ_1 and Φ_2, as would be K and ΔK in (10). Under these circumstances the problem becomes more complicated and we could not use the simple coupled mode theory as developed here.

III. Fiber Couplers with Nonidentical, Untwisted, and Aligned Fibers

The simplest class of couplers to be considered is that made of untwisted fibers $\Phi_i' = 0$, $K_{pi} = 0$, with their major and minor axes aligned with the x and y coordinates, i.e., $\Phi_1 = \Phi_2 = 0$. Under these conditions, $\tilde{E}_x = \tilde{E}_u$, and $\tilde{B} + \tilde{C}$ in (10) becomes

$$\tilde{B} + \tilde{C} = \begin{bmatrix} \beta_1 + \frac{1}{2}\Delta\beta_1 & 0 & K_x & 0 \\ 0 & \beta_1 - \frac{1}{2}\Delta\beta_1 & 0 & K_y \\ K_x & 0 & \beta_2 + \frac{1}{2}\Delta\beta_2 & 0 \\ 0 & K_y & 0 & \beta_2 - \frac{1}{2}\Delta\beta_2 \end{bmatrix}. \tag{13}$$

From the geometry of the coupler or from (10) and (13), it is obvious that there is no coupling between orthogonal polarizations. In fact, such a coupler may be considered as two independent elementary couplers in parallel with an elementary coupler for each polarization

$$\begin{bmatrix} E_{x1}(z) \\ E_{x2}(x) \end{bmatrix} = \exp(-j(\beta_{x1} + \beta_{x2})z/2)\begin{bmatrix} F_{11x} & F_{12x} \\ F_{21x} & F_{22x} \end{bmatrix} \cdot \begin{bmatrix} E_{x1}(0) \\ E_{x2}(0) \end{bmatrix} \tag{14a}$$

$$\begin{bmatrix} E_{y1}(z) \\ E_{y2}(z) \end{bmatrix} = \exp(-j(\beta_{y1} + \beta_{y2})z/2)\begin{bmatrix} F_{11y} & F_{12y} \\ F_{21y} & F_{22y} \end{bmatrix} \cdot \begin{bmatrix} E_{y1}(0) \\ E_{y2}(0) \end{bmatrix} \tag{14b}$$

where

$$\beta_{xi} = \beta_i + \tfrac{1}{2}\Delta\beta_i, \quad (i = 1 \text{ or } 2) \tag{15a}$$

$$\beta_{yi} = \beta_i - \tfrac{1}{2}\Delta\beta_i \tag{15b}$$

$$F_{11x} = F_{22x}^* = \cos(\sqrt{K_x^2 + \delta_x^2}\,z) - j\frac{\delta_x}{\sqrt{K_x^2 + \delta_x^2}}\sin(\sqrt{K_x^2 + \delta_x^2}\,z) = |F_{11x}|e^{-j\theta_{11}} \tag{15c}$$

$$F_{12x} = F_{21x} = -j\frac{K_x}{\sqrt{K_x^2 + \delta_x^2}}\sin(\sqrt{K_x^2 + \delta_x^2}\,z) = |F_{12x}|e^{-j\pi/2} \tag{15d}$$

$$\delta_x = (\beta_{x1} - \beta_{x2})/2 \tag{15e}$$

and F_{ijy} can be written identically with the subscript y replacing x. Except for the phase terms $\exp[-j(\beta_{x1} + \beta_{x2})z/2]$, $\exp[-j(\beta_{y1} + \beta_{y2})z/2]$, (14a) and (14b) are individually equivalent to the expressions obtained by Yariv [27] for the elementary couplers, and collectively, they are equivalent to the expressions derived for the fiber couplers by Sheem and Giallorenzi [1], [2]. For couplers with nonbirefringent fibers, or if only the total power carried by each fiber is of interest, these phase terms are of no consequence. If the fibers are birefringent, and if the fields associated with a polarization and in a given fiber are of interest, then these phase terms have to be accounted for.

To illustrate this point, consider a coupler made of identical fibers $\beta_{x1} = \beta_{x2} = \beta_x$, $\beta_{y1} = \beta_{y2} = \beta_y$, and $\delta_x = \delta_y = 0$. Suppose that a linearly polarized wave with an azimuth θ is incident upon a fiber, referred to as the primary fiber

$$E_{x1}(0) = E_0 \cos\theta \tag{16a}$$

$$E_{y1}(0) = E_0 \sin\theta \tag{16b}$$

and the input to the other fiber, referred to as the tap fiber, is zero,

$$E_{x2}(0) = E_{y2}(0) = 0. \tag{16c}$$

Then the fields and the power in each fiber at an arbitrary point z are [1], [2]

$$\boldsymbol{E}_1(r, \psi, z) = E_0 e^{-j\beta_x z} [\hat{x} \cos K_x z \cos\theta + \hat{y} \cos K_y z \sin\theta\, e^{-j(\beta_y - \beta_x) z}] f(r, \psi) \tag{17a}$$

$$\boldsymbol{E}_2(r, \psi, z) = -jE_0 e^{-j\beta_x z} [\hat{x} \sin K_x z \cos\theta + \hat{y} \sin K_y z \sin\theta\, e^{-j(\beta_y - \beta_x) z}] f(r, \psi) \tag{17b}$$

$$P_1(z) = P_0 [\cos^2 K_x z + \sin(K_x + K_y) z \cdot \sin(K_x - K_y) z \sin^2\theta] \tag{18a}$$

$$P_2(z) = P_0 [\sin^2 K_x z - \sin(K_x + K_y) z \cdot \sin(K_x - K_y) z \sin^2\theta] \tag{18b}$$

where P_0 is the total power fed into the primary fiber at $z = 0$. While the effect of fiber birefringence $\beta_x - \beta_y$ on the output SOP is obvious, it has no effect on the power carried by each fiber. As expected, the total power $P_1 + P_2$ carried by two fibers is conserved. Unless $K_x = K_y$, the fraction of power P_1/P_0 or P_2/P_0 at the point z carried by each fiber would depend on the azimuth of the linearly polarized input. In fact, one can estimate the coupling anisotropy $K_x - K_y$ by measuring P_1/P_0 and P_2/P_0 as functions of θ, provided $K_x \simeq K_y$ which is valid in the weakly guiding approximation of small Δn. Considering a coupler of length L, let $P_{i\max}$ and $P_{i\min}$ be the maximum and minimum output power from fiber i as θ varies. Then it can be shown from (18a) and (18b) that

$$|(K_x - K_y) L| \sim \sin^{-1} \left[\frac{1}{2} \frac{P_{1\max} - P_{1\min}}{\sqrt{P_{1\min} P_{2\max}}}\right] \tag{19a}$$

if

$$\sin(K_x + K_y) L \sin(K_x - K_y) L > 0$$

and

$$|(K_x - K_y) L| \sim \sin^{-1} \left[\frac{1}{2} \frac{P_{1\max} - P_{1\min}}{\sqrt{P_{1\max} P_{2\min}}}\right] \tag{19b}$$

if $\sin(K_x + K_y) L \sin(K_x - K_y) L < 0$. In most cases observed [28] the variation of P_1/P_0 (or P_2/P_0) is only a few percent of the average value of P_1/P_0 (or P_2/P_0), so (19a) and (19b) are approximately equivalent.

The output SOP is quite complicated even for the simple couplers with untwisted and aligned fibers considered here. In general, the output is an elliptically polarized beam, which can be characterized by the visibility VS, the azimuth [i.e., the orientation of the major axis of the polarization ellipse with reference to a given coordinate system], and the sense of rotation [29], [30]. These parameters are experimentally measurable. Usually, the output is examined by an analyzer followed by a power meter. Let $P_{\max}$ and $P_{\min}$ be the maximum and minimum reading of the detector as the analyzer is rotated. Then, the visibility is defined as [30]

$$VS = (P_{\max} - P_{\min})/(P_{\max} + P_{\min}). \tag{20}$$

For a linearly or circularly polarized beam, the visibility is, respectively, 1 or 0. Fig. 2 shows the visibilities on both fibers and power coupled to the tap fiber for a nominally 3 dB coupler with untwisted, aligned, and nonidentical fibers. An examination of (10) and (13) reveals that the results will remain unchanged when all linear dimensions, including the wavelength, are scaled by a constant factor. Therefore, β_{x1} is chosen as 1.0 arbitrarily and all parameters are left dimensionless. Since the fibers are not identical, the variation of the visibility will depend on the fiber involved and on the excitation. In Fig. 2, VS_{ij} and VS_{fi} are plotted as function of θ, where VS_{ij} is the visibility on fiber i when the input power is on fiber j, and VS_{fi} is the visibility on the fiber i when the other fiber is absent (i.e., zero coupling). Note that VS_{11} and VS_{f1} are almost the same, as are VS_{22} and VS_{f2}. In other words, the visibility of the primary fiber is essentially the same as that of the fiber alone and the presence of the tap fiber has only a small effect. Also note that $VS_{12} = VS_{21}$, i.e., the visibilities on the tap fiber are identical no matter which fiber is the primary fiber. Therefore, for nonidentical, aligned fibers without twist, interchange of the input fibers affects only the SOP of the primary fiber, not the SOP of the tap fiber or total power on either fiber. Also shown in Fig. 2 is the fractional power P_t transferred to the tap fiber as a function of θ. The variation of P_t is due to the anisotropy of interfiber coupling as expressed by (19a) and (19b). If $K_x = K_y$, P_t is essentially independent of θ.

Instead of enumerating the variations of the output power and output SOP for all possible input SOP, it is convenient to use Jones' matrices to summarize the relationship between the input and output SOP. A Jones matrix can be written for each path. Once the Jones matrix is known, an ELER can be synthesized. For example, the relation between $(E_{x1}(0), E_{y1}(0))$ and $(E_{x1}(z), E_{y1}(z))$ can be extracted from (14a) and (14b) and arranged as follows:

$$\begin{bmatrix} E_{x1}(z) \\ E_{y1}(z) \end{bmatrix} = \exp(-j(\theta_{11x} + \theta_{11y})/2) \begin{bmatrix} |F_{11x}| & 0 \\ 0 & |F_{11y}| \end{bmatrix} \begin{bmatrix} \exp - j(\theta_{11x} - \theta_{11y})/2 & 0 \\ 0 & \exp + j(\theta_{11x} - \theta_{11y})/2 \end{bmatrix} \cdot \begin{bmatrix} \exp - j(\Delta\beta_1 + \Delta\beta_2) z/4 & 0 \\ 0 & \exp + j(\Delta\beta_1 + \Delta\beta_2) z/4 \end{bmatrix} (\exp - j(\beta_1 + \beta_2) z/2) \begin{bmatrix} E_{x1}(0) \\ E_{y1}(0) \end{bmatrix}. \tag{21}$$

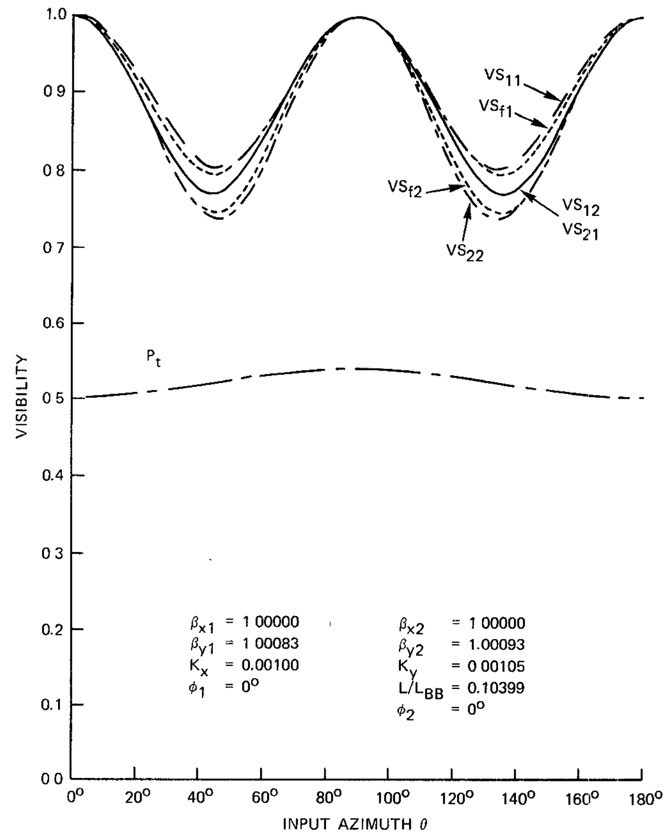

Fig. 2. Polarization characteristics of a coupler with nonidentical, untwisted, and aligned fibers.

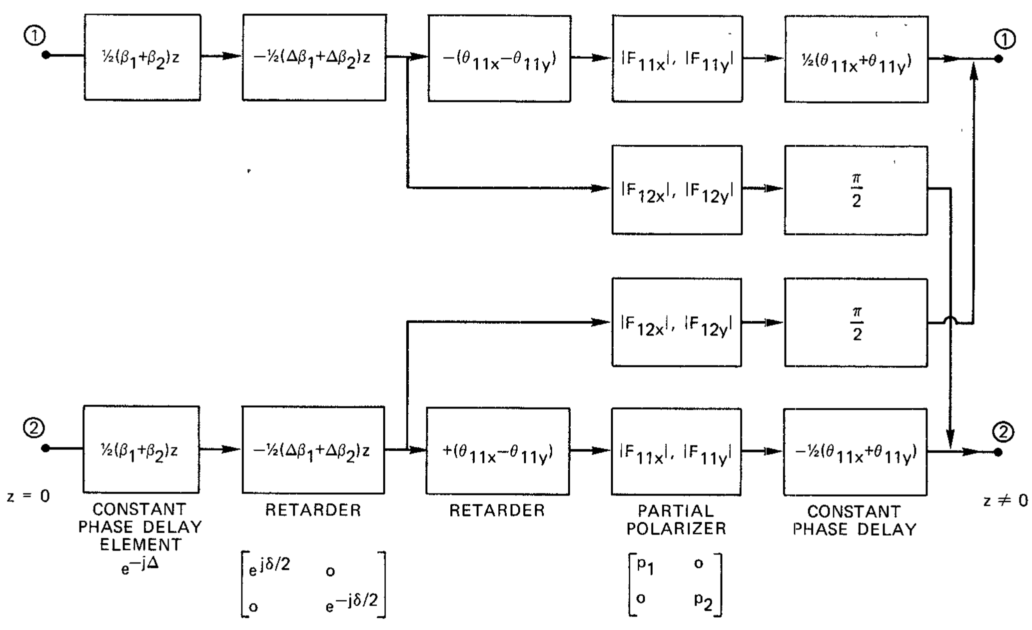

Fig. 3. Equivalent lumped element representation for couplers with nonidentical, untwisted, and aligned fibers.

These exponential terms and the (2×2) matrices represent, respectively, a constant phase delay element $((\theta_{11x} + \theta_{11y})/2)$, a partial polarizer with unequal principal transmittances, a linear retarder with retardation $-(\theta_{11x} - \theta_{11y})$, another retarder with retardation $-(\Delta\beta_1 + \Delta\beta_2) z/2$, and another delay element $(\beta_1 + \beta_2) z/2$ [23], [24], [30]. The ELER for this path, together with that of the other coupler paths are shown in Fig. 3.

Note that for the simple case considered here, no rotator is involved and the principal axes of all lumped elements are aligned with the x-axis. If $K_x = K_y$, and if the fibers are identical, we have $\theta_{11x} = \theta_{11y} = 0$, and $|F_{11x}| = |F_{11y}|$, $|F_{12x}| = |F_{12y}|$. Then the retarder and the constant phase delay element associated with $\theta_{11x} \pm \theta_{11y}$ disappear and the partial polarizers become simple isotropic absorbers. The ELER is greatly simplified as shown in Fig. 4. The elements enclosed in the dashed boxes can be identified as the ELER for the untwisted fibers. The effects of interfiber coupling are

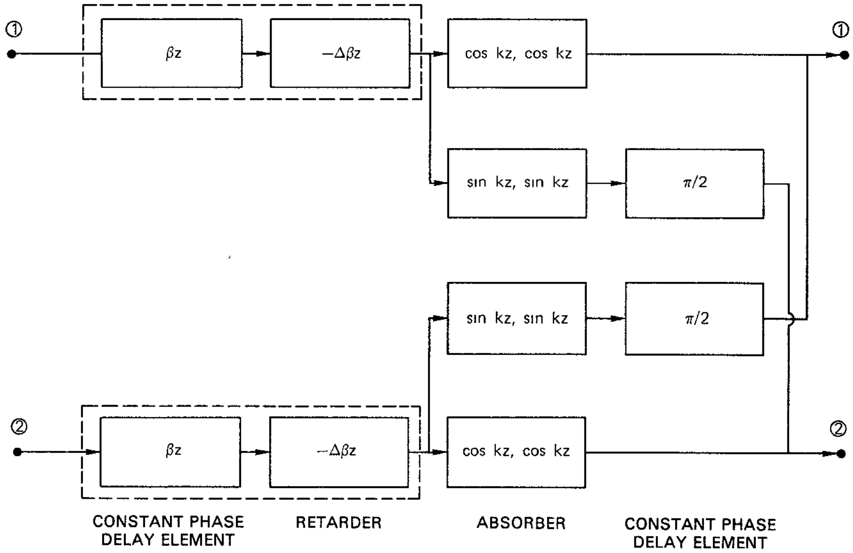

Fig. 4. Equivalent lumped element representation for couplers with identical, untwisted, and aligned fibers.

reflected only in the isotropic absorbers and $\pi/2$ phase delay elements. Thus, for isotropic coupling with untwisted, identical, and aligned fibers, the SOP of the output of the coupler is identical to the output SOP of the fibers with the same birefringence and length.

IV. Fiber Couplers with Identical, Untwisted, and Unaligned Fibers

Of all the assumptions made in the last sections, the assumption of alignment, i.e., $\Phi_1 = \Phi_2 = 0$ is probably the most unrealistic one. It is therefore desirable to understand the effect of misalignment ($\Phi_1 \neq \Phi_2$) on the polarization characteristics of the coupler. To reduce the complexity of the problem, we assume that the fibers are identical ($\beta_1 = \beta_2 = \beta$, $\Delta\beta_1 = \Delta\beta_2 = \Delta\beta$) and interfiber coupling is isotropic ($\Delta K = 0$). For untwisted fibers, Φ_i is a constant ϕ_i, and K_{pi} vanishes. Then $\tilde{C} = 0$ and $\tilde{B}$ becomes

$$\tilde{B} = \begin{bmatrix} \beta + \frac{1}{2}\Delta\beta & 0 & K\cos(\phi_1 - \phi_2) & K\sin(\phi_1 - \phi_2) \\ 0 & \beta - \frac{1}{2}\Delta\beta & -K\sin(\phi_1 - \phi_2) & K\cos(\phi_1 - \phi_2) \\ K\cos(\phi_1 - \phi_2) & -K\sin(\phi_1 - \phi_2) & \beta + \frac{1}{2}\Delta\beta & 0 \\ K\sin(\phi_1 - \phi_2) & K\cos(\phi_1 - \phi_2) & 0 & \beta - \frac{1}{2}\Delta\beta \end{bmatrix}. \tag{22}$$

The coupled-mode equations (10) and (22) may be further simplified by defining symmetric (E_{us}, E_{vs}) and antisymmetric (E_{ua}, E_{va}) modes

$$\begin{bmatrix} E_{us} \\ E_{vs} \\ E_{ua} \\ E_{va} \end{bmatrix} = \frac{1}{2} \begin{bmatrix} 1 & 0 & 1 & 0 \\ 0 & 1 & 0 & 1 \\ 1 & 0 & -1 & 0 \\ 0 & 1 & 0 & -1 \end{bmatrix} \begin{bmatrix} E_{u1} \\ E_{v1} \\ E_{u2} \\ E_{v2} \end{bmatrix}. \tag{23}$$

Since the symmetric and antisymmetric modes are uncoupled, analytic solutions may be written immediately which in turn can be transformed to $\tilde{E}_u$

$$\begin{bmatrix} E_{u1}(z) \\ E_{v1}(z) \\ E_{u2}(z) \\ E_{v2}(z) \end{bmatrix} = \frac{1}{2} e^{-j\beta z} \begin{bmatrix} F_{11} + F_{33} & F_{14} + F_{32} & F_{11} - F_{33} & F_{32} - F_{14} \\ F_{14} + F_{32} & F_{11}^* + F_{33}^* & F_{14} - F_{32} & F_{33}^* - F_{11}^* \\ F_{11} - F_{33} & F_{14} - F_{32} & F_{11} + F_{33} & -F_{14} - F_{32} \\ F_{32} - F_{14} & F_{33}^* - F_{11}^* & -F_{14} - F_{32} & F_{33}^* + F_{11}^* \end{bmatrix} \begin{bmatrix} E_{u1}(0) \\ E_{v1}(0) \\ E_{u2}(0) \\ E_{v2}(0) \end{bmatrix} \tag{24}$$

where

$$F_{11} = \cos Xz - j\,\frac{\Delta\beta + 2K\cos(\phi_1 - \phi_2)}{2X}\sin Xz \tag{25}$$

$$F_{14} = j\,\frac{K\sin(\phi_1 - \phi_2)}{X}\sin Xz \tag{26}$$

$$F_{33} = \cos Yz - j\,\frac{\Delta\beta - 2K\cos(\phi_1 - \phi_2)}{2Y}\sin Yz \tag{27}$$

$$F_{32} = -j\,\frac{K\sin(\phi_1 - \phi_2)}{Y}\sin Yz \tag{28}$$

and

$$X = [(K\cos(\phi_1 - \phi_2) + \tfrac{1}{2}\Delta\beta)^2 + K^2\sin^2(\phi_1 - \phi_2)]^{1/2} \tag{29}$$

$$Y = [(K\cos(\phi_1 - \phi_2) - \tfrac{1}{2}\Delta\beta)^2 + K^2\sin^2(\phi_1 - \phi_2)]^{1/2}. \tag{30}$$

To relate $\tilde{E}_x(z)$ with $\tilde{E}_x(0)$, it is only necessary to use (24) in conjunction with (7). More specifically, the relationship between $(E_{x1}(z), E_{y1}(z))$ and $(E_{x1}(0), (E_{y1}(0))$ is

$$\begin{bmatrix} E_{x1}(z) \\ E_{y1}(z) \end{bmatrix} = \frac{1}{2} e^{-j\beta z} \begin{bmatrix} \cos\phi_1 & -\sin\phi_1 \\ \sin\phi_1 & \cos\phi_1 \end{bmatrix} \cdot \begin{bmatrix} F_{11}+F_{33} & F_{14}+F_{32} \\ F_{14}+F_{32} & F_{11}^*+F_{33}^* \end{bmatrix} \begin{bmatrix} \cos\phi_1 & \sin\phi_1 \\ -\sin\phi_1 & \cos\phi_1 \end{bmatrix} \cdot \begin{bmatrix} E_{x1}(0) \\ E_{y1}(0) \end{bmatrix}. \tag{31}$$

The first and third square matrices correspond to rotators. It can be shown that the second matrix is a product of a constant $2\sqrt{1-P_t}$, and unitary matrix

$$\begin{bmatrix} F_{11}+F_{33} & F_{14}+F_{32} \\ F_{14}+F_{32} & F_{11}^*+F_{33}^* \end{bmatrix} = 2\sqrt{1-P_t} \cdot \begin{bmatrix} (F_{11}+F_{33})/(2\sqrt{1-P_t}) & (F_{14}+F_{32})/(2\sqrt{1-P_t}) \\ (F_{14}+F_{32})/(2\sqrt{1-P_t}) & (F_{11}^*+F_{33}^*)/(2\sqrt{1-P_t}) \end{bmatrix}$$

where

$$P_t = \sin^2 (X+Y) z/2 - \frac{XY - (K^2 - \Delta\beta^2/4)}{2XY} \sin Xz \sin Yz \tag{32}$$

is the fraction of power transferred to the tap fiber. The constant factor $\sqrt{1-P_t}$ corresponds to an isotropic absorber with two equal principal transmittances. The unitary matrix is equivalent to a retarder placed between two rotators [24]. Thus, all elements of the ELER representing the relationship between $(E_{x_1}(0), E_{y1}(0))$ are known. Fig. 5 displays the ELER for isotropic coupling with untwisted, unaligned, and identical fibers. Also given there are expressions for all elements of the ELER. In the special case $\phi_1 = \phi_2 = 0$, Figs. 4 and 5 become identical, as expected.

The effect of misalignment can be understood as follows: when $\phi_1 = \phi_2$, E_{us}, E_{ua}, E_{vs}, and E_{va} are four uncoupled orthogonal modes with propagation constant $\beta \pm \frac{1}{2}\Delta\beta \pm K$. When the fibers are misaligned, the modes become coupled, E_{us} with E_{va}, and E_{ua} with E_{vs}, with coupling constants $\pm K \sin(\phi_1 - \phi_2)$. The propagation constants are also changed, thus affecting the retardations δ_{11}, δ_{12} defined in Fig. 5 and the transmittance of the absorbers. However, the unitary character of the transfer matrices remains unchanged.

To study the polarization characteristics of couplers with unaligned fibers, we consider the evolution of the output SOP with a linearly polarized input [(16a), (16b)]. As the azimuth θ of the input polarization changes, the visibility of the output would vary between 1 and a minimum value. To be specific, 3 dB couplers are considered. For a given fiber birefringence $\Delta\beta$, misalignment $\phi_1 - \phi_2$, and coupler length $z = L$, a value for K can be determined such that $P_t = \frac{1}{2}$. From $\Delta\beta$, $\phi_1 - \phi_2$, L, and the value of K so obtained, δ_{11} and δ_{12} can be computed, which in turn leads to the minimum visibility at some value of θ. The results are shown in Fig. 6 which displays the minimum visibility on the primary fiber $(VS_p)_{\min}$ and on the tap fiber $(VS_t)_{\min}$ as functions of L/L_{BB}. Also shown there is the minimum visibility $(VS_f)_{\min}$ due to the birefringent fiber alone. Note that the $(VS_p)_{\min}$ curve follows closely to that of $(VS_f)_{\min}$, particularly in the region where L/L_{BB} is small. As L/L_{BB} increases, the effects of interfiber coupling and misalignment become more evident. The difference between $(VS_t)_{\min}$ and $(VS_f)_{\min}$ is quite noticeable especially in the region $L/L_{BB} \sim 0.5$. The effect of $\phi_1 - \phi_2$ on $(VS_p)_{\min}$ and $(VS_t)_{\min}$ has also been examined. It is interesting to note that when $\phi_1 - \phi_2 = \pm 90°$, the output on the tap fiber is always linearly polarized, $(VS_t)_{\min} = 1$, for any linearly polarized input. Mathematically, this can be deduced from the fact that $\delta_{12} = 0$ when $\phi_1 - \phi_2 = \pm 90°$. Physically, it may be understood as follows. When $\phi_1 - \phi_2 = \pm 90°$, the fast mode of fiber 1 is coupled with the slow mode of fiber 2, and vice versa. Thus, the coupling between one set of modes (i.e., the fast mode of fiber 1 with the slow mode of fiber 2) is exactly the same as the coupling between the other set (i.e., the slow mode of fiber 1 with the fast mode of fiber 2). Then the output SOP on the tap fiber is exactly the same as the input SOP. Conceptually, this leads to the possibility of constructing couplers, with polarization maintaining properties on the tap fiber, from any birefringent fibers. Of course, the fiber alignment is critical and fibers have to be handled in a way that no extraneous birefringence is introduced.

V. Fiber Couplers with Twisted Fibers

In this section, couplers with twisted fibers are considered. We assume that the fibers are twisted uniformly and with identical twist rate ξ

$$\Phi_i(z) = \xi z + \phi_i. \tag{33}$$

ϕ_i is the orientation of fiber i at $z = 0$. Then $\Phi_1 - \Phi_2 = \phi_1 - \phi_2$. Since K_{pi} is proportional to the twist rate [15]-[18] $K_{p1} = K_{p2} = K_p$. Under these conditions, and with $\tilde{C} = 0$, (10) again reduces to a set of simultaneous equations with constant coefficients. To identify the effect of twisting, we begin by considering a simplified situation: couplers with identical and aligned fibers ($\beta_1 = \beta_2 = \beta$, $\Delta\beta_1 = \Delta\beta_2 = \Delta\beta$, $\phi_1 = \phi_2$). Then the term $K \sin(\Phi_1 - \Phi_2)$ in (11) vanishes. Again symmetric and antisymmetric modes can be defined as in (23) and analytic solutions become available.

$$\begin{bmatrix} E_{u1}(z) \\ E_{v1}(z) \\ E_{u2}(z) \\ E_{v2}(z) \end{bmatrix} = e^{-j\beta z} \begin{bmatrix} G_{11}\cos Kz & G_{12}\cos Kz & -jG_{11}\sin Kz & -jG_{12}\sin Kz \\ -G_{12}\cos Kz & G_{11}^*\cos Kz & jG_{12}\sin Kz & -jG_{11}^*\sin Kz \\ -jG_{11}\sin Kz & -jG_{12}\sin Kz & G_{11}\cos Kz & G_{12}\cos Kz \\ jG_{12}\sin Kz & -jG_{11}^*\sin Kz & -G_{12}\cos Kz & G_{11}^*\cos Kz \end{bmatrix} \begin{bmatrix} E_{u1}(0) \\ E_{v1}(0) \\ E_{u2}(0) \\ E_{v2}(0) \end{bmatrix} \tag{34}$$

where

$$G_{11} = \cos Zz - j\frac{\Delta\beta}{2Z}\sin Zz$$

$$G_{12} = \frac{\xi - K_p}{Z}\sin Zz$$

$$Z = [(\xi - K_p)^2 + \Delta\beta^2/4]^{1/2}.$$

Following the procedure established in the previous sections,

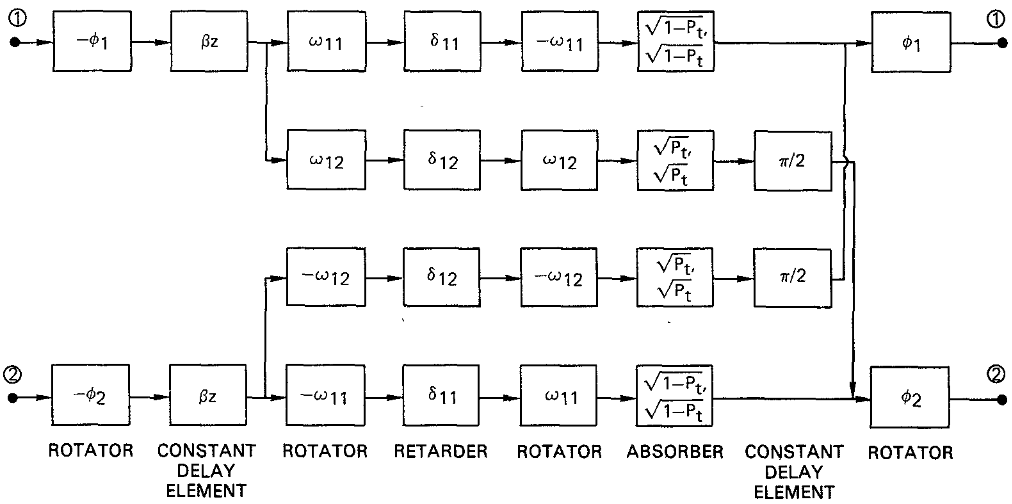

$$\left.\begin{matrix}\omega_{11}\\ \omega_{12}\end{matrix}\right\} = -\tfrac{1}{2}\tan^{-1}\frac{2K\sin(\phi_1-\phi_2)\,[Y\sin Xz \mp X\sin Yz]}{[\Delta\beta+2K\cos(\phi_1-\phi_2)]\,Y\sin Xz \pm [\Delta\beta-2K\cos(\phi_1-\phi_2)]\,X\sin Yz}$$

$$\delta_{11} = 2\cos^{-1}\left[(\cos Xz + \cos Yz)/(2\sqrt{1-P_t})\right]$$

$$\delta_{12} = 2\sin^{-1}\left[(\cos Xz - \cos Yz)/(2\sqrt{P_t})\right]$$

Fig. 5. Equivalent lumped element representation for couplers with identical, untwisted, and unaligned fibers.

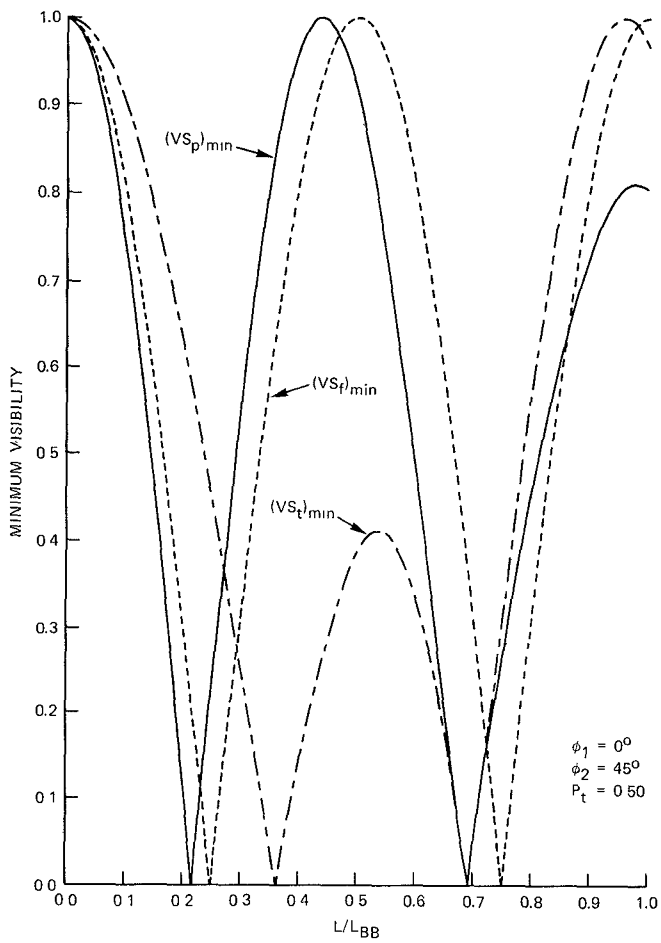

Fig. 6. Polarization characteristics of a nominally 3 dB coupler with identical, untwisted, and unaligned fibers.

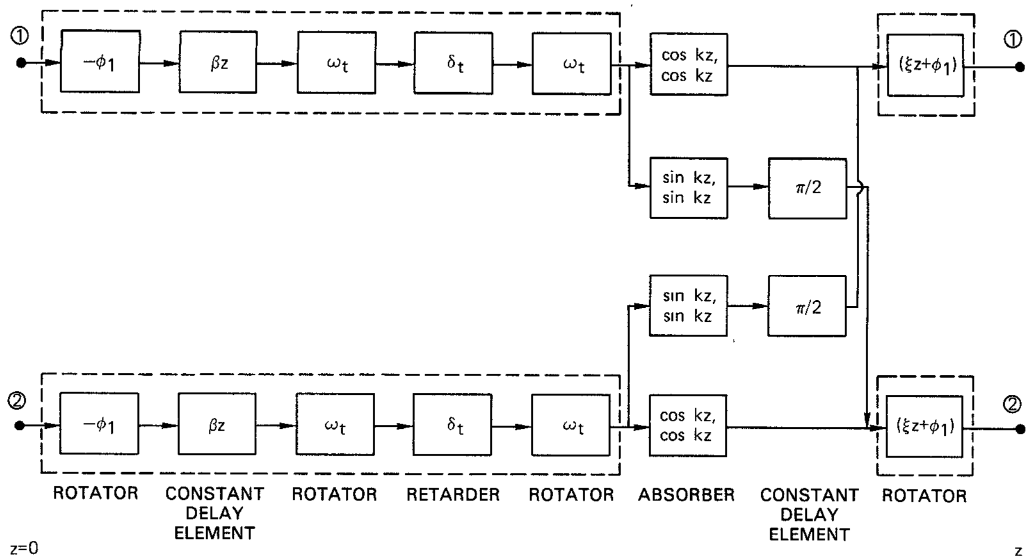

$$\omega_t = -\frac{1}{2}\tan^{-1}\left[\frac{\xi - k_{pa}}{Z}\tan Zz\right]$$

$$\delta_t = -2\sin^{-1}\left[\frac{\Delta\beta/2}{z}\sin Zz\right]$$

Fig. 7. Equivalent lumped element representation for couplers with identical, twisted, and aligned fibers.

the ELER can be obtained (Fig. 7). The lumped elements enclosed by the dashed lines are exactly those for uncoupled twisted fibers alone. The effect of interfiber coupling between the fibers is reflected only by the presence of the isotropic absorbers ($\cos Kz$ or $\sin Kz$) and the $\pi/2$ phase delay element in the crossover branch. This is reminiscent of isotropic couplers with untwisted, identical, and aligned fibers. In particular, it is noted that the retardance is

$$\delta_t = -2\sin^{-1}\left[\frac{\Delta\beta}{2Z}\sin Zz\right]. \tag{35}$$

If the fibers are not twisted, ($\xi = K_p = 0$), $\delta_t = -\Delta\beta z$ which is precisely the retardance given in Fig. 4 for the case without twist. As the twist rate increases, the retardance δ_t oscillates with a decreasing amplitude. In fact, for couplers with heavily twisted fibers, i.e., $|\xi - K_p| \gg \Delta\beta$, (35) reduces to

$$\delta_t \simeq -\Delta\beta z\,\frac{\sin(|\xi - K_p|z)}{|\xi - K_p|z} \tag{36}$$

which shows how a high twist rate overrides the effect of the linear birefringence $\Delta\beta$. In this high twist rate limit, the normal modes of the coupler become circularly polarized in opposite directions [25], resulting in a linearly polarized output for a linearly polarized input. This suggests another approach to making a coupler which preserves linear polarization, providing sufficient twist could be imparted to the fibers over the interaction length of the coupler.

We cannot treat the case of nonidentical twist in fiber couplers because the $\Phi_2 - \Phi_1$ terms in (10) become z-dependent and an analytical solution is no longer possible. We would expect that the isotropic feature of the absorbers in Fig. 7 would be lost in an amount depending on the difference in the twist rates. However, the high twist limit, as discussed above, should still qualitatively apply.

As long as the fibers are twisted equally, a general algorithm may be used to study (10), even though the fibers are nonidentical ($\beta_1 \neq \beta_2$, $\Delta\beta_1 \neq \Delta\beta_2$) and/or unaligned ($\phi_1 \neq \phi_2$). Let Λ_i be the ith eigenvalue and $\tilde{P}_i$ be the corresponding eigenvector of $\tilde{B}(i = 1\text{-}4)$. Then $\tilde{Q}$ and $\tilde{P}$ can be constructed

$$\tilde{Q} = \begin{bmatrix} \exp - j\Lambda_1 z & 0 & 0 & 0 \\ 0 & \exp - j\Lambda_2 z & 0 & 0 \\ 0 & 0 & \exp - j\Lambda_3 z & 0 \\ 0 & 0 & 0 & \exp - j\Lambda_4 z \end{bmatrix} \tag{37}$$

$$\tilde{P} = [\tilde{P}_1 \;\; \tilde{P}_2 \;\; \tilde{P}_3 \;\; \tilde{P}_4] \tag{38}$$

and the solution of (10), subject to the initial condition $\tilde{E}_u(0)$, can be written as

$$\tilde{E}_u(z) = \tilde{P}\tilde{Q}\tilde{P}^{-1}\tilde{E}_u(0). \tag{39}$$

In terms of the stationary coordinate systems

$$\tilde{E}_x(z) = \tilde{T}(\xi z + \phi_1, \xi z + \phi_2)\tilde{P}\tilde{Q}\tilde{P}^{-1}\tilde{T}(-\phi_1, -\phi_2)\tilde{E}_x(0). \tag{40}$$

This general algorithm has been used to calculate the polarization characteristics of couplers with twisted but nonidentical and unaligned fibers. As the previous case the visibility approaches unity in the high twist limit. This is illustrated in Fig. 8 where visibilities for primary VS_{11} and tap VS_{12} fibers in a nominal 3 dB coupler are plotted versus the input azimuth θ for increasing twist rates. The parameters used correspond to couplers with a coupling length of 4.0 mm, constructed from birefringent fiber with L_{BB} = 7.5 cm, and twisted at a rate of 0, 0.1, 0.5, and 1 turns/cm. The initial misalignment is $\phi_2 - \phi_1 = 45°$. It is interesting to note that the mechanical strength of glass would limit the maximum twist rate to 10 turns/cm

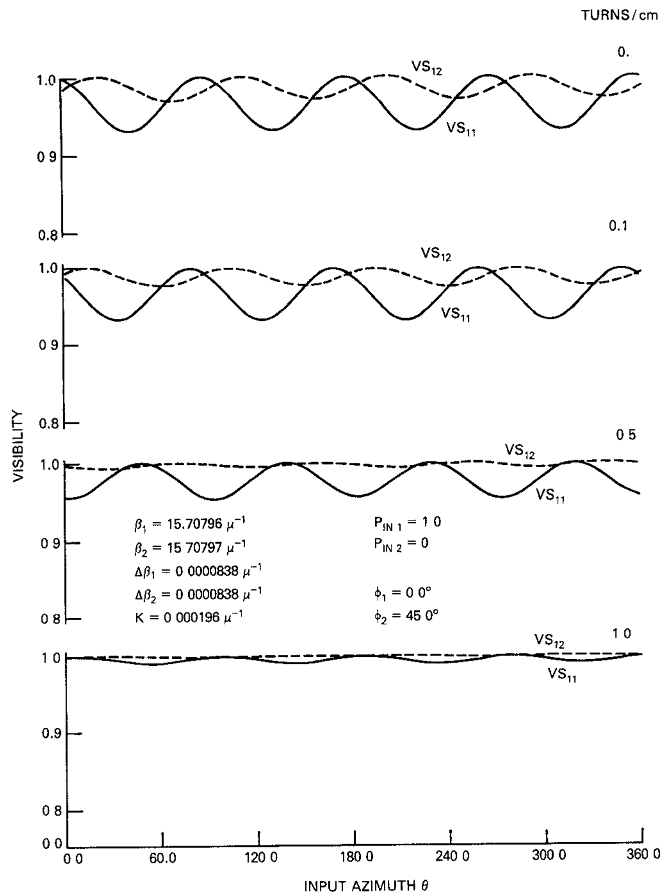

Fig. 8. Effect of twisting on the polarization characteristics of couplers with nonidentical, twisted, and unaligned fibers.

[31] and it has also been reported that fibers may be twisted by 1 turn/cm without breaking [32].

The effect of the initial misalignment $\phi_2 - \phi_1$ on couplers with twisted fibers has also been investigated. We find similar behavior to the effect of alignment without twist, as discussed in Section IV. The tap fiber visibility approaches unity as $|\phi_2 - \phi_1| \approx 90°$, while the primary fiber visibility is not significantly affected.

It would be desirable to have an ELER for the couplers with twisted, but nonidentical or nonaligned, fibers as well. The equivalent representations for $\tilde{T}(-\phi_1, -\phi_2)$ and $\tilde{T}(\xi z + \phi_1, \xi z + \phi_2)$ are simply a rotator at each end of the fibers. However, the ELER for $\tilde{P}\tilde{Q}\tilde{P}^{-1}$ is quite complicated. $\tilde{P}\tilde{Q}\tilde{P}^{-1}$, a 4×4 matrix, can be subdivided into four Jones matrices, with one for each of the four paths between the input and output ports. Numerical calculation showed that these Jones matrices are not unitary nor are they the products of a constant and a unitary matrix. An exact ELER for each path would consist of a partial polarizer, two retarders, and a rotator, according to Hurwitz and Jones' theorem [24].

VI. Discussion and Conclusions

There are two additional complications in the fabrication of real couplers that we have not considered in our analysis. First is the addition of induced nonuniform birefringence caused by the fabrication of the coupler to the intrinsic uniform fiber birefringence which we have modeled. Considering the fabrication methods employed in all the couplers of references [1]-[9], it seems that none would be free from these effects. Twisting, fusing, polishing, and fixing with epoxy or glass-gel would all induce or alter the intrinsic birefringence of the fiber. Additionally, even the very low birefringence fibers fabricated by perform spinning are susceptible to this difficulty. Second is the effect of the birefringence in the fiber leads, which are required to access the coupling region. In principle the fiber leads can be modeled by lumped element representations and placed in series with that of the coupler to characterize the transmission matrix of the coupler as a whole. If the induced or intrinsic birefringence of the leads is substantial, however, they cannot be neglected.

Some experimental results have been reported by Sheem and co-workers [2], [4] and additional data have also been obtained by Koo and Villarruel [28]. These experimental results are in qualitative agreement with those presented in this work. Since the precise rate of twisting in the coupling region is not known and it is difficult to separate the effects of the fiber leads and birefringence induced by packaging from the contributions from the coupler, a quantitative comparison is not feasible. However, we expect that the treatment provided here will aid in the interpretation of future experimental work.

In the previous sections, the following three idealized classes of couplers were studied in detail:

1) couplers with nonidentical, untwisted, and aligned fibers with anisotropic interfiber coupling, ($\beta_1 \neq \beta_2$, $\Delta\beta_1 \neq \Delta\beta_2$, $\xi_1 = \xi_2 = 0, \phi_1 = \phi_2 = 0, K_x \neq K_y$),

2) couplers with identical, untwisted, misaligned fibers with isotropic interfiber coupling ($\beta_1 = \beta_2, \Delta\beta_1 = \Delta\beta_2, \xi_1 = \xi_2 = 0, \phi_1 \neq \phi_2, K_x = K_y$), and

3) couplers with identical, uniformly and equally twisted aligned fibers, and isotropic interfiber coupling ($\beta_1 = \beta_2$, $\Delta\beta_1 = \Delta\beta_2, \xi_1 = \xi_2 \neq 0, \phi_1 = \phi_2, K_x = K_y$).

From these studies, the effects due to nonidentical fibers, anisotropic interfiber coupling, misalignment, and fiber twisting have been identified. An exact equivalent lumped element representation (ELER) was obtained for each class of coupler and these representations are particularly helpful in understanding the polarization characteristics of the fiber coupler. If we consider identical fibers with isotropic coupling for the cases of aligned axes 1) and aligned axes with equal twist 3), we see from Figs. 4 and 7 that coupling has no effect on the SOP in the fibers whatsoever. The polarizer elements are isotropic. As noted previously a partial polarizer with two equal principal transmittances is really a simple isotropic absorber [23], [24]. For these two classes of couplers the SOP is determined completely by the intrinsic and induced (by twist) birefringence in the fibers. When identical fibers are unaligned [case 2)], the situation is more complicated in that now the SOP is perturbed by the act of coupling itself. However, in this case, the polarizing element in the lumped model is still isotropic so that the power coupled is still independent of input polarization (for $K_x \simeq K_y$). We show in Fig. 6 that in the worst case, for small values of L/L_{BB}, the output visibilities are of the same order as the worst case visibility in a single fiber with the same birefringence. Finally, in the apparently simple case of Fig. 3, where nonidentical fibers with real anisotropic coupling are aligned, we have the most complicated case with the output SOP complicated by the presence of the partial polarizers in the ELER, which represents polarization dependent coupling. However, we know these effects will be small because real couplers, to date, are made from fiber from the same sample and the anisotropy in K is small, 5 percent or less [9]. Although our examples are obviously oversimplified, we use a similar argument to extend our results to a real coupler, i.e., we expect in a real coupler that the deviations from our assumptions will be relatively small and that we can conclude that the primary determinant of the SOP in a fiber coupler is the intrinsic and induced birefringence in the fibers used to make the coupler. Our assumption of identical twist is the weakest in this regard since identical twist is not likely to occur in a real coupler unless deliberately induced.

In each of the equivalent lumped element representations the power coupling fraction is represented either by isotropic absorbers in an idealized case, or by partial polarizers in more generally anisotropic cases. We note from the work of Jones *et al.* [23], [24] that these seemingly complicated representations for each path can be replaced by a single rotator, a single retarder, and an isotropic absorber, in the cases where the transfer matrix is unitary, and by two retarders, an anisotropic partial polarizer, and a rotator, when the transfer matrix is not unitary.

We have identified two special cases where fiber couplers maintain linear polarization for arbitrary input azimuth. These include the case of 90° misalignment where the tap fiber has a constant unity visibility, and the case of high uniform twist where both outputs approach unity visibility in the high twist limit.

It is of interest to consider the implications of our results to couplers fabricated with high-birefringence or polarization maintaining fibers. Although we have restricted our analysis to cases where the index or geometrical ellipticity is not too large, our results should at least qualitatively apply to high birefringence fibers as well. The advantage of high birefringence would be that polarization would be maintained even in the presence of weak induced birefringences. It is obvious from Fig. 5 that the fibers would have to be aligned at 0°, in which case the linear input would also have to be aligned, or at 90°, in which case only the tap fiber would have unity visibility. Probably the largest experimental problem, after alignment, would be to avoid the relaxation of the high birefringence during coupler fabrication.

Acknowledgment

The authors wish to thank K. P. Koo, S. C. Rashleigh, and C. A. Villarruel for helpful discussions, and T. G. Giallorenzi for suggesting this problem.

References

[1] S. K. Sheem and T. G. Giallorenzi, "Single-mode fiber-optical power divider: Encapsulated etching technique," *Opt. Lett.*, vol. 4, pp. 29–31, 1979.
[2] ——, "Polarization effects on single-mode optical fiber sensors," *Appl. Phys. Lett.*, vol. 35, pp. 914–917, 1978.
[3] D. C. Tran, K. P. Koo, and S. K. Sheem, "Single-mode fiber directional couplers fabricated by twist-etching techniques (stabilization)," *IEEE J. Quantum Electron.*, vol. QE-17, pp. 988–981, June 1981.
[4] S. K. Sheem, H. F. Taylor, R. P. Moeller, and W. K. Burns, "Propagation characteristics of single-mode evanescent field couplers," *Appl. Opt.*, vol. 20, pp. 1056–1059, 1981.
[5] J. F. Liao and J. T. Boyd, "Single-mode fiber coupler," *Appl. Opt.*, vol. 20, pp. 2731–2734, 1981.
[6] C. A. Villaurruel and R. P. Moeller, "Fused single-mode fiber access couplers," *Electron. Lett.*, vol. 17, pp. 243–244, 1981.
[7] C. A. Villarruel, R. P. Moeller, and W. K. Burns, "Tapped tee single-mode data distribution system," *IEEE J. Quantum Electron.*, vol. QE-17, pp. 941–946, June 1981.
[8] R. A. Bergh, G. Kotler, and H. J. Shaw, "Single-mode fiber optic directional coupler," *Electron. Lett.*, vol. 16, pp. 260–261, 1980.
[9] M. Digonnet and H. J. Shaw, "Analysis of a tunable single-mode optical fiber coupler," *IEEE J. Quantum Electron.*, vol. QE-18, pp. 746–754, Apr. 1982.
[10] G. Schiffner, H. Schneider, and G. Schoner, "Double-core single-mode optical fiber as directional couplers," *J. Appl. Phys.*, vol. 23, pp. 41–45, 1980.
[11] G. Schoner and G. Schiffner, "Coupling properties of a double-core single-mode fiber," *Siemens Forsch.-u Entwickl.*, vol. 10, pp. 172–178, 1981.
[12] D. Marcuse, *Theory of Dielectric Optical Waveguides.* New York: Academic, 1974.
[13] V. Ramaswamy, W. G. French, and R. D. Standley, "Polarization characteristics of noncircular core single-mode fibers," *Appl. Opt.*, vol. 17, pp. 3014–3017, 1978.
[14] P. Kaminow, J. R. Simpson, H. M. Presby, and J. B. MacChesney, "Strain birefringence in single-polarization Germanosillicate optical fibers," *Electron. Lett.*, vol. 15, pp. 677–680, 1979.

[15] R. Ulrich, S. C. Rashleigh, and W. Eickhoff, "Bending induced birefringence in single-mode fibers," *Opt. Lett.*, vol. 5, pp. 273–275, 1980.
[16] R. Ulrich and A. Simon, "Polarization optics of twisted single-mode fibers," *Appl. Opt.*, vol. 18, pp. 2241–2251, 1978.
[17] A. M. Smith, "Birefringence induced by bends and twists in single-mode optical fiber," *Appl. Opt.*, vol. 19, pp. 2606–2610, 1980.
[18] W. Eickhoff, Y. Yen, and R. Ulrich, "Wavelength dependence of birefringence in single-mode fiber," *Appl. Opt.*, vol. 20, pp. 3428–3435, 1981.
[19] I. P. Kaminow, "Polarization in optical fibers," *IEEE J. Quantum Electron.*, vol. QE-17, pp. 15–22, Jan. 1981.
[20] J. I. Sakai and T. Kimura, "Birefringence and polarization characteristics of single-mode optical fibers under elastic deformations," *IEEE J. Quantum Electron.*, vol. QE-17, pp. 1041–1051, June 1981.
[21] A. J. Barlow, J. J. Ramskov-Hansen, and D. N. Payne, "Birefringence and polarization mode-dispersion in spun single-mode fibers," *Appl. Opt.*, vol. 20, pp. 2962–2968, 1981.
[22] M. Monerie and L. Jeunhomme, "Polarization mode coupling in long single-mode fibers," *Opt. Quantum Electron.*, vol. 12, pp. 449–461, 1980.
[23] R. C. Jones, "A new calculus for the treatment of optical systems: I. Description and discussion of the calculus," *J. Opt. Soc. Amer.*, vol. 31, pp. 488–493, 1941.
[24] H. Hurwitz and R. C. Jones, "A new calculus for the treatment of optical systems: II. Proof of three general equivalence theorems," *J. Opt. Soc. Amer.*, vol. 31, pp. 493–499, 1941.
[25] P. McIntyre and A. W. Snyder, "Light propagation in twisted anisotropic media: Application to photoreceptors," *J. Opt. Soc. Amer.*, vol. 68, pp. 149–157, 1978.
[26] R. Vanclooster and P. Phariseau, "The coupling of two parallel dielectric fibers, Parts I and II," *Physics*, vol. 47, pp. 485–514, 1970.
[27] A. Yariv, "Coupled-mode theory for guided-wave optics," *IEEE J. Quantum Electron.*, vol. QE-9, pp. 919–933, 1973.
[28] K. P. Koo and C. A. Villarruel, private communications, 1981.
[29] M. Born and E. Wolf, *Principles of Optics*, 6th ed. New York: Pergamon, 1980, pp. 24–32.
[30] W. A. Shurcliff, *Polarized Light, Production and Use*. Cambridge, MA: Harvard University Press, 1962.
[31] A. J. Barlow and D. N. Payne, "Polarization maintenance in circularly birefringent fibers," *Electron. Lett.*, vol. 17, pp. 388–389, 1981.
[32] L. Jeunhomme and M. Monerie, "Polarization-maintaining single-mode fiber cable design," *Electron. Lett.*, vol. 16, pp. 921–922, 1980.

Chin-Lin Chen received the B.S.E.E. degree from National Taiwan University, Taipei, China, in 1958, the M.S. degree from North Dakota State University, Fargo, in 1961, and the Ph.D. degree from Harvard University, Cambridge, MA, in 1965.

From 1965 to 1966, he was a Research Fellow in the Division of Engineering and Applied Physics, Harvard University. In 1966, he joined the School of Electrical Engineering, Purdue University, West Lafayette, IN, as an Assistant Professor. He is currently a Professor of Electrical Engineering. From 1981 to the present he has been on sabbatical leave at the Vitreous State Laboratory, The Catholic University of America, Washington, DC, and the Naval Research Laboratory, Washington, DC. His research interests are in the areas of scattering and diffraction of electromagnetic waves, antenna radiation, surface acoustic wave filters and cavities, and the integrated and fiber optical components.

Dr. Chen is a member of Sigma Xi, Eta Kappa Nu, the American Society for Engineering Education, and the U.S. National Committee for the International Union of Radio Science.

William K. Burns (M'80) was born in Philadelphia, PA, in June 1943. He received the B.S. degree in engineering physics from Cornell University, Ithaca, NY, in 1965, and the M.S. and Ph.D. degrees in applied physics from Harvard University, Cambridge, MA, in 1967 and 1971, respectively. His thesis research was in nonlinear optics.

During 1971 he was a staff member at Arthur D. Little, Inc., Cambridge, MA, where he contributed to various laser-related studies and surveys. Since 1972 he has been a Research Physicist at the Naval Research Laboratory, Washington, DC. He is presently Head of the Optical Waveguide Section of the Optical Techniques Branch. His research interests include integrated optics, single-mode fiber optics, and the application of single-mode technology to communications, sensors, and signal processing.

Dr. Burns is a member of the Optical Society of America.